Biotechnol Lett (2021) 43:2035–2043
https://doi.org/10.1007/s10529-021-03169-z

ORIGINAL RESEARCH PAPER

Modification of an engineered *Escherichia coli* by a combinatorial strategy to improve 3,4-dihydroxybutyric acid production

Yidi Liu · Xinlei Mao · Baoqi Zhang · Jinping Lin · Dongzhi Wei

Received: 12 April 2021 / Accepted: 5 August 2021 / Published online: 26 August 2021

Abstract
Objectives 3,4-Dihydroxybutyric acid (3,4-DHBA) is a multifunctional C4 platform compound widely used for the synthesis of various materials, including pharmaceuticals. Although, a biosynthetic pathway for 3,4-DHBA production has been developed, its low yield still precludes large-scale use. Here, a heterologous four-step biosynthetic pathway was established in recombinant *Escherichia coli* (*E. coli*) using a combinatorial strategy.
Results Several aldehyde dehydrogenases (ALDHs) were screened, using in vitro enzyme assays, to identify suitable catalysts for the dehydrogenation of 3,4-dihydroxybutanal (3,4-DHB) to 3,4-DHBA. A pathway containing glucose dehydrogenase (*Bs*GDH) from *Bacillus subtilis*, D-xylonate dehydratase (YagF) from *E. coli*, benzoylformate decarboxylase (*Pp*MdlC) from *Pseudomonas putida* and ALDH was introduced into *E. coli*, generating 3.04 g/L 3,4-DHBA from D-xylose (0.190 g 3,4-DHBA/g D-xylose). Disruption of competing pathways by deleting *xylA*, *ghrA*, *ghrB* and *adhP* contributed to an 87% increase in 3,4-DHBA accumulation. Expression of a fusion construct containing *Pp*MdlC and YagF enhanced the 3,4-DHBA titer, producing the highest titer and yield reported thus far (7.71 g/L; 0.482 g 3,4-DHBA/g D-xylose).
Conclusions These results showed that deleting genes from competing pathways and constructing fusion proteins significantly improved the titer and yield of 3,4-DHBA in engineered *E. coli*.

Keywords 3,4-DHBA · D-Xylose · Competing pathway · Fusion protein · *E. coli*

Supplementary Information The online version contains supplementary material available at https://doi.org/10.1007/s10529-021-03169-z.

Y. Liu · X. Mao · B. Zhang · J. Lin (✉) · D. Wei
State Key Laboratory of Bioreactor Engineering, New World Institute of Biotechnology, East China University of Science and Technology, Shanghai 200237, People's Republic of China
e-mail: jplin@ecust.edu.cn

Y. Liu
e-mail: yidiliu33@foxmail.com

X. Mao
e-mail: 995698729@qq.com

B. Zhang
e-mail: zhangbaoqi1992@163.com

D. Wei
e-mail: dzwei@ecust.edu.cn

Introduction

3,4-Dihydroxybutyric acid (3,4-DHBA) is an important C4 compound containing hydroxyl and carboxyl groups that can be modified to produce antibiotics (Choi et al. 2015), α- and β-amino acids and peptides (Sang et al. 2010). 3-Hydroxy-γ-butyrolactone

(3HBL), the lactone of 3,4-DHBA, is also a multifunctional chiral building block for various chiral drugs, including the antilipemic agent atorvastatin (Brower et al. 1992), neurotransmitter L-carnitine (Tetrahedron 1990), HIV protease inhibitor Amprenavir (Kim E E 1995), dermatological medicine 12-HETE (Corey E J 1978), and anti-cancer drug aplysistatin (Shieh H M 1982).

Currently, 3,4-DHBA is mainly produced using an H_2O_2-catalyzed reaction between glucose and alkali metal hydroxides conducted at 70 °C for 24 h (Hollingsworth 1994), or from the hydrocyanation and hydrolyzation of *R*-3-chloro-1,2-propanediol (Inoue et al. 1991). However, these approaches usually generate low yields, in addition to involving harsh reaction conditions, complex product purification processes, high costs, and environmental pollution. Therefore, the biosynthesis of 3,4-DHBA from renewable sources has attracted considerable attention. For instance, efforts have been made to produce 3,4-DHBA by microbial fermentation.

There have been no reports of a natural pathway for 3,4-DHBA production. The first de novo biosynthesis of 3,4-DHBA, developed in *E. coli*, involved a six-step enzymatic reaction using glucose, and acyl-CoA as a substrate and acyl donor (Liu et al. 2009; Schweiger and Buckel 1984; Taguchi et al. 2008). After optimizations by Dhamankar et al., a yield of 0.7 g/L 3,4-DHBA (0.105 g 3,4-DHBA/g glucose) was achieved (Dhamankar et al. 2014). However, the numerous reaction steps, low catalytic efficiency, and low yield make this pathway unsuitable for industrial production.

D-xylose has a high proportion of lignocellulose, which is as the most abundant renewable biomass in energy production found in nature (Choi et al. 2014; Kawaguchi et al. 2016). A novel five-step biosynthetic pathway for the generation of 3,4-DHBA from D-xylose has been constructed in *E. coli* (Wang et al. 2017), in which xylose is catalyzed to 3,4-DHBA by double dehydrogenation followed by oxidation, dehydration and decarboxylation. In shake flask experiments, the titer of 3,4-DHBA has achieved 1.27 g/L (0.079 g 3,4-DHBA/g D-xylose), with 0.18 g/L (0.012 g 1,2,4-butanetriol/g D-xylose) of by-product of 1,2,4-butanetriol (BTO). This yield has remained low because of the lack of highly active enzymes to efficiently decarboxylate 2-keto-3-deoxy-D-xylonate and dehydrogenate 3,4-DHB, and because intermediate products are consumed by competing pathways.

In this study, a four-step biosynthetic pathway using D-xylose as a precursor was developed to produce 3,4-DHBA (Fig. 1). First, several aldehyde dehydrogenases (ALDHs) were screened and characterized to identify potential catalysts suitable for maximizing 3,4-DHBA accumulation. Second, competing pathways were disrupted by deleting *xylA*, *ghrA*, *ghrB* and *adhP*. Finally, a fusion construct containing *Pp*MdlC and YagF was created to improve the titer of 3,4-DHBA. This study provided novel strategies for achieving a high titer and yield of 3,4-DHBA.

Methods and materials

Strains, plasmids and culture conditions

The *E. coli* BL21(DE3) was used for expressing, purifying target proteins and producing 3,4-DHBA. Strains used in this study were showed in Table 1. The plasmids pET28a and pACYC184 were used for cloning and expressing the target genes. *E. coli* cells were cultured at 37 °C in lysogeny broth medium added with appropriate concentration antibiotics. And plasmids in this study were showed in Table S1.

Construction of plasmids

The primers sequences used are listed in Table S2. pE01 harboring *yagF* from *E. coli* and *PpmdlC* from *P. putida* was constructed. Similarity, pE04, pE05 and pE06 carrying *gdh* from *B. subtilis* and different ALDH genes, respectively.

The gene segment of T7 promoter-*PpmdlC* was amplified from pET28a harboring *PpmdlC*. The backbone of pET28a harboring *yagF* with *Spe*I and *Sal*I of multiple cloning site was obtained by PCR. A 5 nm rigid α-helical ER/K linker(Sivaramakrishnan and Spudich 2011) was selected to connected to these two segments to create a new plasmid which carrying a fusion construct (Fig. S1).

The disruption of competing pathways

The disruption of competing pathway was accomplished by CRISPR-Cas9. The donor DNA was

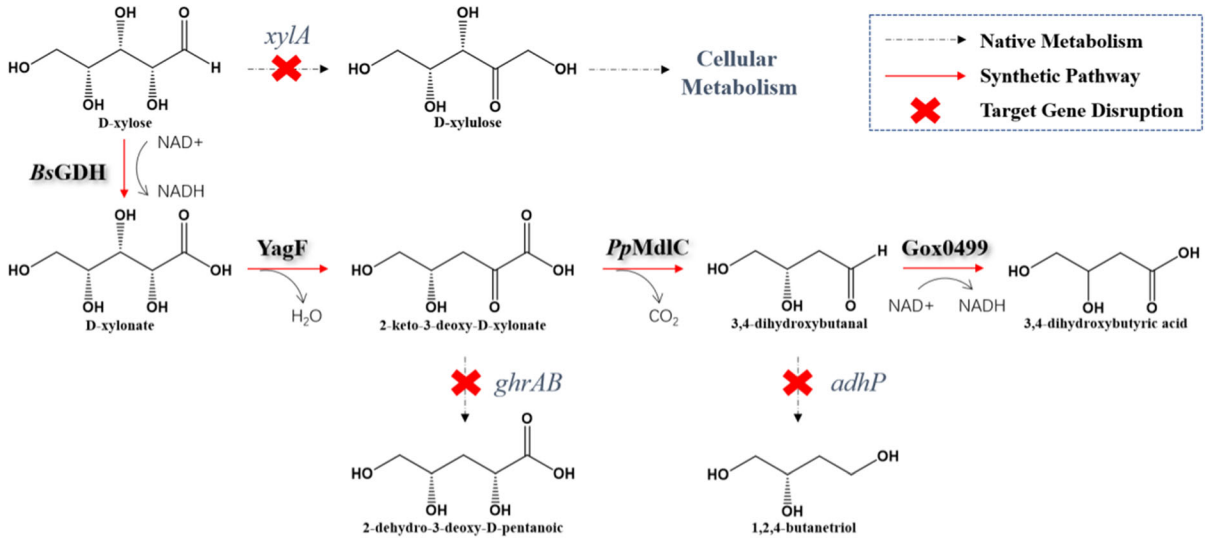

Fig. 1 The pathway from xylose to produce 3,4-DHBA in *E. coli*. Enzymes: *Bs*GDH: glucose dehydrogenase; YagF: D-xylonate dehydratase; *Pp*MdlC: decarboxylase; ALDH: aldehyde dehydrogenase. Genes: *xylA* encoding xylose isomerase; *ghrA*, *ghrB* encoding glyoxylate reductases, respectively; *adhP* encoding ethanol dehydrogenase

Table 1 *E. coli* strains used in this study

Strains	Description	Source
E. coli BL21(DE3)	Expression, purification and production	Our laboratory
E0-E01-A01	*E. coli* BL21(DE3) carrying pE01 (pET28a harboring *E. coli yagF* and *P. putida PpmdlC*) and pA01 (pACYC184 harboring *E. coli yneI* and *B. subtilis gdh*)	This study
E0-E01-A02	*E. coli* BL21(DE3) carrying pE01 and pA02 (pACYC184 harboring *G. oxydans gox0499* and *B. subtilis gdh*)	This study
E0-E01-A03	*E. coli* BL21(DE3) carrying pE01 and pA03 (pACYC184 harboring *G. oxydans gox1122* and *B. subtilis gdh*)	This study
E1-E01-A02	*E. coli* BL21(DE3) Δ*xylA* carrying pE01 and pA02	This study
E2-E01-A02	*E. coli* BL21(DE3) Δ*xylA* Δ*ghrA* carrying pE01 and pA02	This study
E3-E01-A02	*E. coli* BL21(DE3) Δ*xylA* Δ*ghrA* carrying pE01 and pA02	This study
E4-E01-A02	*E. coli* BL21(DE3) Δ*xylA* Δ*ghrA* Δ*ghrB* carrying pE01 and pA02	This study
E5-E01-A02	*E. coli* BL21(DE3) Δ*xylA* Δ*ghrA* Δ*ghrB* Δ*adhP* carrying pE01 and pA02	This study
E5-E02-A02	*E. coli* BL21(DE3) Δ*xylA* Δ*ghrA* Δ*ghrB* Δ*adhP* carrying pE02 (pET28a harboring fusion gene of *E. coli yagF* and *P. putida PpmdlC*) and pA02	This study

connected by overlapping PCR from 500 bp upstream and downstream homologous arm. The *E. coli* BL21(DE3) carrying pCas vector was inoculated in 30 °C and then added into 10 mM arabinose for inducing the expression of Cas9. When OD_{600} reached 0.5–0.6, the *E. coli* cells were arranged on ice for 30 min. After washed by 10% glycerol sterile three times, it was split into 100 μL per tube. The competent cells carrying pCas were mixed with 100 ng pTargetT vector and 400 ng donor DNA to have an electrotransformation (2.5 kV, 200 Ω, 25 μF) with an electrical shock time within 5 ms. Then they were cultivated into 30 °C and confirmed by colony PCR.

E. coli cells were cultured in 30 °C with addition of 0.5 mM IPTG overnight to eliminate pTargetT series because IPTG could induce the other sgRNA, which

targets one PAM site of pTargetT. The pCas vector could be cured by cultivating it in 37 °C to remove because its temperature sensitivity.

Protein expression and purification

E. coli cells were cultured at 37 °C until the OD_{600} was approximately 0.6–0.8, and then 0.2 mM IPTG was used to induce target proteins expression at 20 °C for 16 h. Then the cells were collected by centrifugated at 8000 rpm for 10 min, washed by 0.9% NaCl twice and resuspended in appropriate volume PB solution at pH 7.5 (20 mM Na_2HPO_4 and NaH_2PO_4). The resuspended cells were centrifuged to collect the supernatants for purification after ultrasonication. The supernatants were filtered, loaded in the pre-equilibrated (20 mM imidazole, pH 7.5) Ni-chelating column with and then washed with different concentration of imidazole (20 mM and 50 mM, pH 7.5). The bound proteins including YneI, Gox0499 and Gox1122 would be eluted by 250 mM imidazole (pH 7.5). The protein samples were then put into dialysate (20 M PB solution, 200 mM NaCl and 5% glycerol, pH 7.5) overnight, and then identified by 12% SDS-PAGE.

Enzymes activity assay

The in vitro enzyme assays of the fusion protein and tandem enzyme reaction system containing YagF and *Pp*MdlC were performed in a 50 mM PB solution (pH 7.5) containing 20 mM D-xylonate, 10 mM $MgCl_2$, 1 mM TPP, and 1 mM NAD^+. The reaction mixture was incubated at 30 °C for 5 min to allow the accumulation of 3,4-DHB produced by the five-fold excess of YagF, *Pp*MdlC or the YagF and *Pp*MdlC fusion protein. The absorbance of NADH at 340 nm was measured after 1 mM YneI was added to the reaction.

The in vitro enzyme assay of NAD^+-dependent YneI, Gox0499, and Gox1122 activity was performed in a 50 mM PB solution (pH 7.5) containing 20 mM D-xylonate, 10 mM $MgCl_2$, 1 mM TPP, 1 mM NAD^+, and a five-fold excess of YagF and *Pp*MdlC. The reaction mixture was incubated at 30 °C for 5 min to allow the accumulation of 3,4-DHB, after which 1 mM YneI, 1 mM Gox0499, and 1 mM Gox1122 were added. The NADH absorbance at 340 nm was then measured.

Whole-cell catalysis for 3,4-DHBA production

Whole-cell catalysis was performed in 20 mL scale, containing 20 g/L of D-xylose, 50 mM PB solution (pH 7.5), 50 g/L of *E. coli* cells, 2 mM TPP, 2 mM NAD^+, 10 mM Mg^{2+} at 30 °C. The products were sampled about 1 mL in every 12 h and analyzed via HPLC.

Analytical methods

Metabolite analysis was performed by HPLC on a Transgenomic 87H3 column, using refractive-index detection (RID). The mobile phase was 0.08 N H_2SO_4 with a flow rate of 0.38 mL/min. The temperatures of the RID detector and column were 35 °C. HPLC–MS was used to distinguishing 3,4-DHBA from the supernatants of reaction (Fig. S2). 3,4-DHBA ($C_4H_8O_4$) was corresponded to the peak of 119.03 Da under the negative ion mode.

Results and discussion

Selection of enzymes for 3,4-DHBA dehydrogenation

The biosynthetic pathway for producing 3,4-DHBA from D-xylose comprises four steps. First, *Bs*GDH from *B. subtilis* catalyzes D-xylose to produce D-xylonate (Li et al. 2017). Second, YagF from *E. coli* converts D-xylonate to 2-keto-3-deoxy- D-xylonate. Third, *Pp*MdlC from *P. putida* produces 3,4-dihydroxybutanal (3,4-DHB) from 2-keto-3-deoxy-D-xylonate(Sun et al. 2016).

Finally, YneI from *E. coli* is used to convert 3.4-DHB to 3,4-DHBA(Wang et al. 2017). However, YneI generates 3,4-DHBA and BTO as byproducts. To obtain highly active oxidases to minimize the production of BTO, we identified two NAD^+-dependent ALDHs (Gox0499 and Gox1122 from *Gluconobacter oxydans*) and compared their catalytic activity with that of YneI, using in vitro enzyme assays performed in cell lysates. Gox0499 had a higher specific activity (4.26 U/mg protein) than YneI (2.67 U/mg protein) and Gox1122 (2 U/mg protein).

To evaluate the catalytic activity of the enzymes in vivo, the plasmids pE01 (carrying *yagF* and *PpmdlC*), pA01 (carrying *yneI* and *gdh*), pA02

(carrying *gox0499* and *gdh*), and pA03 (carrying *gox1122* and *gdh*) were constructed to assemble the entire 3,4-DHBA biosynthetic pathway in *E. coli* BL21(DE3). Figure 2A shows the SDS-PAGE results of target proteins expressed by the strains E0-E01-A01, E0-E01-A02, and E0-E01-A03 after cultivation and target induction. The expression levels of *Bs*GDH, YagF, and *Pp*MdlC were the same among the three strains, but those of the ALDHs differed; Gox1122 levels were higher than those of YneI and Gox0499.

Next, strains E0-E01-A01, E0-E01-A02, and E0-E01-A03 were used for whole-cell catalysis to produce 3,4-DHBA. As seen in Fig. 2B, strain E0-E01-A02 produced approximately 3.04 g/L 3,4-DHBA (0.190 g 3,4-DHBA/g D-xylose) after a 60 h whole-cell catalytic process, with 0.56 g/L of the by-product BTO. Compared with E0-E01-A01 and E0-E01-A03, E0-

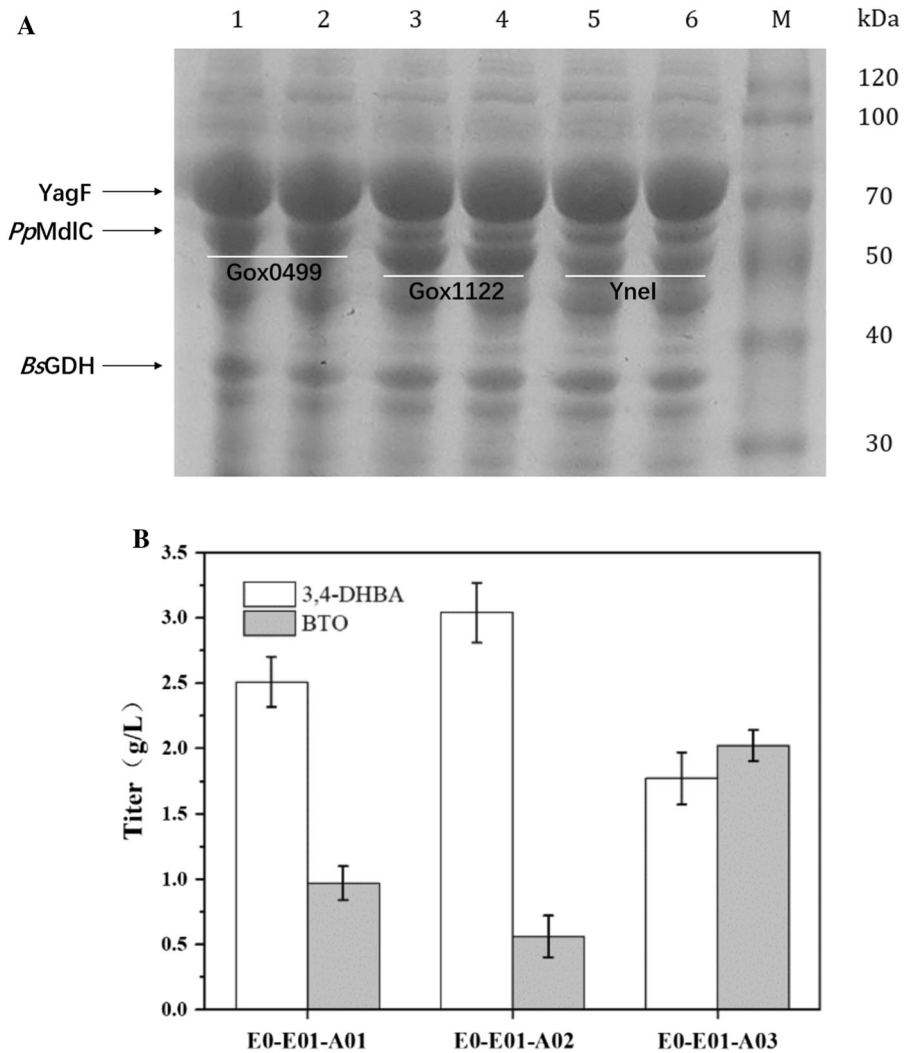

Fig. 2 Selection of ALDHs for 3,4-DHBA production. **A** SDS-PAGE analysis of E0-E01-A01, E0-E01-A02 and E0-E01-A03. Lane 1: whole cell of E0-E01-A02; Lane 2: crude extract of E. coli E0-E01-A02; Lane 3: whole cell of E0-E01-A03; Lane 4: crude extract of E0-E01-A03; Lane 5: whole cell of E0-E01-A01; Lane 6: crude extract of E0-E01-A01; M: protein molecular weight marker. **B** Several strains were constructed to compare the titer of 3,4-DHBA. The highest titer of 3,4-DHBA (3.04 g/L; yield of 0.190 g 3,4-DHBA/g D-xylose) was produced by E0-E01-A02 containing *Bs*GDH, YagF, *Pp*MdlC and Gox0499, while the lowest titer of BTO was obtained, which means the Gox0499 has the highest oxidative activity and lowest reductive activity among these three ALDHs. These three reactions were performed in 20 mL scale, containing 20 g/L of D-xylose, 50 mM PB solution (pH 7.5), 2 mM TPP, 2 mM NAD^+, 10 mM Mg^{2+} at 30 °C

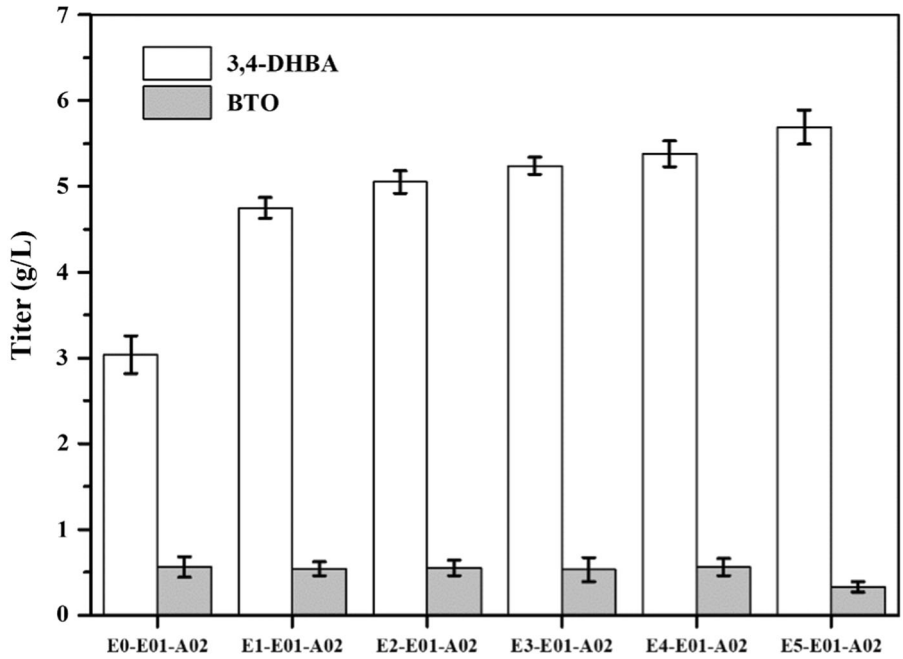

Fig. 3 Disruptions of genes of *xylA*, *ghrA*, *ghrB* and *adhP* for improving titer of 3,4-DHBA. Titer of 3,4-DHBA was produced by different engineered strains. Reaction conditions and systems are as shown in Fig. 2B

E01-A02 had the highest and lowest titers of 3,4-DHBA and BTO, respectively. Since Gox0499 was shown to be the most efficient enzyme for the dehydrogenation of 3,4-DHB, functioning at a lower level of protein expression, it was selected for 3,4-DHBA production.

Disruption of competing pathways to improve 3,4-DHBA titer

To improve the titer of 3,4-DHBA synthesized from D-xylose, several genes in competing pathways were deleted using CRISPR/Cas9. Xylose isomerase, encoded by *xylA*, catalyzes the production of D-xylulose from D-xylose. D-xylulose then enters the pentose phosphate pathway, facilitating bacterial growth and metabolism. 2-keto-3-deoxy-D-xylonate aldolases, expressed by *yagE* and *yjhG* of the Dahms pathway, always consumed the intermediate product 2-keto-3-deoxy-D-xylonate in *E. coli* (Valdehuesa et al. 2014). A search of the NCBI database showed that the genome of *E. coli* BL21(DE3) did not contain *yagE* or *yjhG*. However, *ghrA* and *ghrB* of *E. coli* BL21(DE3) were found to encode glyoxylate reductase, which consumes the intermediate product 2-keto-3-deoxy-D-xylonate. In addition, the ALDH encoded by *adhP* has a high level of reduction activity, favoring the production of the by-product BTO from 3,4-DHB (Wang et al. 2017).

After knocking out these competing genes, the *xylA*-deficient strain E1-E01-A02; *xylA* and *ghrA* double-deficient strain E2-E01-A02; *xylA* and *ghrB* double-deficient strain E3-E01-A02, *xylA*, *ghrA* and *ghrB* triple-deficient strain E4-E01-A02, and *xylA*, *ghrA*, *ghrB* and *adhP* quadruple-deficient strain E5-E01-A02 were constructed using CRISPR/Cas9. There was no significant difference in the expression of target proteins among the engineered strains (Fig. S3). This indicated that the deletion of *xylA*, *ghrA*, *ghrB* and *adhP* had no effect on the expression of target proteins in the host cell.

E1-E01-A02 produced a 56% higher 3,4-DHBA titer than E0-E01-A02 (Fig. 3). This showed that the deletion of *xylA* minimized the by-product formation of D-xylulose and increased the flux of the conversion of D-xylose to D-xylonate. The 3,4-DHBA titers produced by E2-E01-A02, E3-E01-A02, and E4-E01-A02 were 5.05, 5.24, and 5.38 g/L, respectively. This result indicated that the knockout of *ghrA* and *ghrB* increased the titer of 3,4-DHBA, but this effect

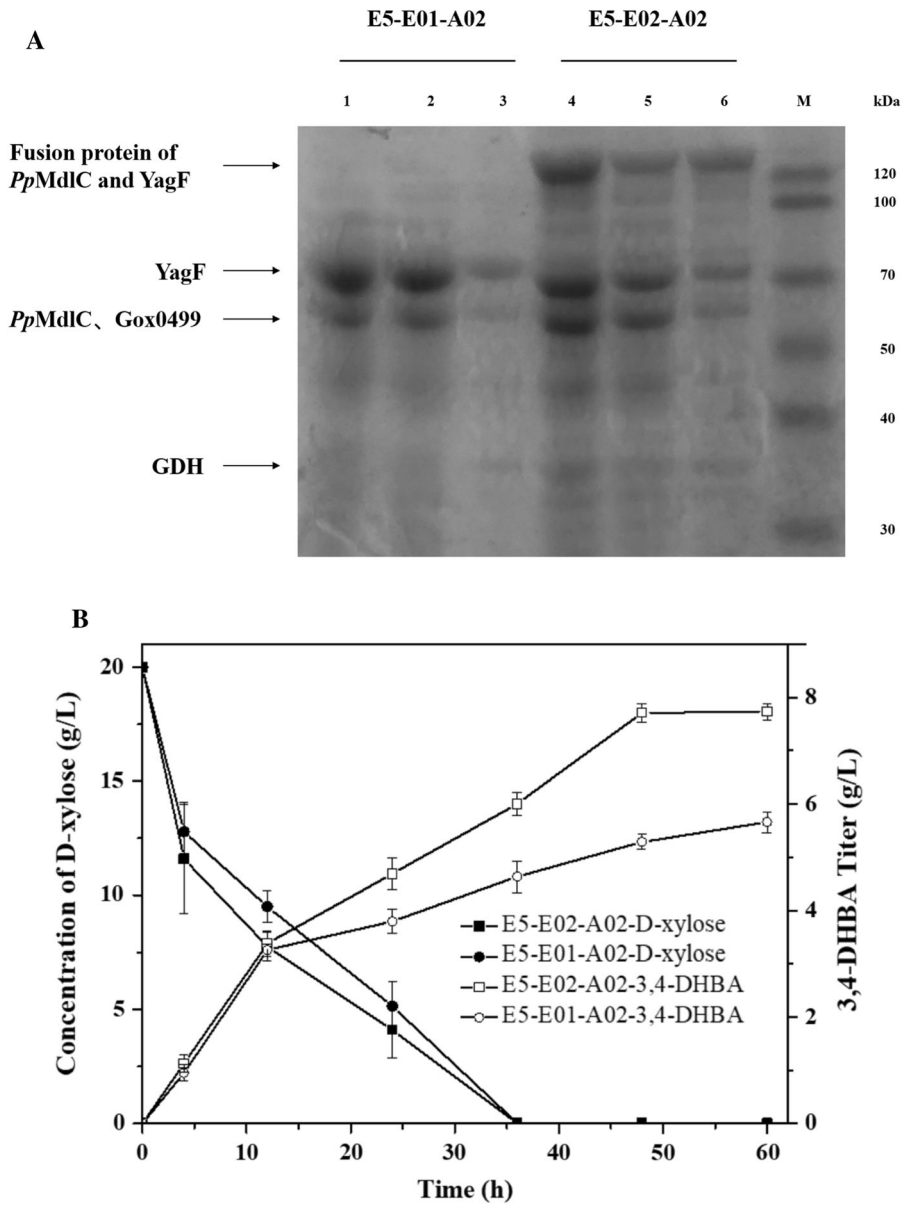

Fig. 4 Protein fusion of *Pp*MdlC and YagF to improve 3,4-DHBA production. **A** The SDS-PAGE analysis of E5-E01-A02 and E5-E02-A02. Lane 1: whole cell of E5-E01-A02; Lane 2: crude extract of E5-E01-A02; Lane 3: precipitate of E5-E01-A02; Lane 4: whole cell of E5-E02-A02; Lane 5: crude extract of E5-E02-A02; Lane 6: precipitate of E5-E02-A02; M: protein molecular weight marker. **B** E5-E02-A02 was engineered to have *Pp*MdlC and YagF fusion expression to enhance the reaction efficiency. The highest titer of 3,4-DHBA was 7.71 g/L (yield of 0.482 g 3,4-DHBA/g D-xylose) produced by E5-E02-A02, with same reaction condition and system as Fig. 2B

was negligible. The 3,4-DHBA titer produced by the *xylA*, *ghrA*, *ghrB* and *adhP* quadruple-deficient strain E5-E01-A02 was 5.69 g/L, and the BTO titer decreased from 0.56 g/L to 0.33 g/L, suggesting that *adhP* disruption was essential for 3,4-DHBA production. E5-E01-A02 produced the highest titer, at 5.69 g/L (0.356 g 3,4-DHBA/g D-xylose), 87% higher than that produced by E0-E01-A02. We concluded that disruption increased the titer and yield of 3,4-DHBA.

Construction of a fusion protein containing PpMdlC and YagF to increase carbon flux toward the 3,4-DHBA pathway

*Pp*MdlC was the rate-limiting enzyme in this pathway because of its lower catalytic activity (Wang et al. 2017; Zhong et al. 2019), which causes the accumulation of intermediate products and consumption by competing pathways. Fusion proteins that serve as multifunctional enzymes can be constructed (Chen et al. 2016); previous studies have shown that enhancing the spatial proximity of enzymes by constructing fusion proteins can increase catalytic efficiency and the titer of products in multi-enzyme cascade reaction (Albertsen et al. 2011; Lu et al. 2006; Ryosuke et al. 2018). Here, a fusion construct containing *Pp*MdlC and YagF with a 5 nm rigid α-helical ER/K motif was created, and the resulting recombinant plasmid pE02 was co-transformed into *E. coli* BL21(DE3) among with pA02 to generate the engineered strain E5-E02-A02.

The protein expression of *Pp*MdlC and YagF in E5-E02-A02 was lower than that in the engineered strain E5-E01-A02, which harbored plasmids pE01 and pA02 (Fig. 4A). Meanwhile, a new protein of over 120 kDa was observed, indicating that the fusion protein expressing *Pp*MdlC and YagF was constructed successfully. The catalytic activity of *Pp*MdlC and YagF was compared to that of a tandem enzymatic reaction system containing PpMdlC and YagF by monitoring the change in NADH absorbance at 340 nm, with D-xylonate used as a substrate and Gox0499 used to catalyze the subsequent reaction in the cascade. The catalytic activity of the fusion protein containing *Pp*MdlC and YagF was only 1.09 U/g wet cell, compared to 2.53 U/g wet cell produced by the tandem enzymatic reaction system containing *Pp*MdlC and YagF.

The 3,4-DHBA titer was further compared between the engineered strains E5-E01-A02 and E5-E02-A02. The rates of consumption of the substrate D-xylose in these two engineered strains were similar (Fig. 4B). Additionally, the 3,4-DHBA titer in E5-E02-A02 (7.71 g/L; 0.482 g 3,4-DHBA/g D-xylose) accumulated was higher and that in E5-E01-A02, and the reaction in E5-E02-A02 ended 12 h earlier. E5-E02-A02 exhibited a higher titer and yield of 3,4-DHBA than E5-E01-A02 at a lower level of *Pp*MdlC and YagF enzymatic activity. The close spatial proximity of *Pp*MdlC and YagF might have prevented the diffusion of the intermediate 2-keto-3-deoxy-D-xylonate, indicating that the constructed variant containing fusion enzymes effectively regulated catalytic efficiency. At the same time, there are no differences between E5-E01-A02 and E5-E02-A02 on cell growth (Fig. S4).

Conclusion

In this study, we developed a four-step enzymatic reaction pathway in *E. coli* to efficiently produce 3,4-DHBA from D-xylose. In addition to YagF from *E. coli* and *Pp*MdlC from *P. putida*, used in the 3,4-DHBA biosynthetic pathway reported previously (Valdehuesa et al. 2014), *Bs*GDH from *B. subtilis* was selected to catalyze the conversion of D-xylose to D-xylonate. Additionally, the ALDH Gox0499 from *G. oxydans* which exhibited higher activity than YneI from *E. coli* (Taguchi et al. 2008) was chosen to catalyze the conversion of 3,4-DHB to 3,4-DHBA, resulting in a higher titer of 3,4-DHBA and a lower titer of the by-product BTO. *E. coli* strains containing recombinant plasmids were modified by deleting genes in competing pathways and introducing fusion construct expressing *Pp*MdlC and YagF. Whole cells of the engineered strain E5-E02-A02 produced 7.71 g/L 3,4-DHBA (0.482 g 3,4-DHBA/g D-xylose), the highest titer and yield reported to date.

Acknowledgements This work was supported by the Natural Science Foundation of Shanghai (No. 19ZR1412700), the Fundamental Research Funds for the Central Universities (No. 22221818014), and partially supported by the Open Funding Project of the State Key Laboratory of Bioreactor Engineering.

Supplementary Information Supplementary Table 1—List of plasmids this study.

Supplementary Table 2—List of primer sequences this study.

Supplementary Figure 1—Schematic illustration of this fusion construct.

Supplementary Figure 2—HPLC-MS in negative ion mode for 3,4-DHBA verification by strain E0-E01-A01. 3,4-DHBA (C4H8O4) was corresponded to the retention time of 1.0 min and the peak of 119.03 Da.

Supplementary Figure 3—SDS-PAGE analysis of target proteins of the engineered strains. Lane 1: whole cell of E0-E01-A02; Lane 2: whole cell of E1-E01-A02; Lane 3: whole cell of E2-E01-A02; Lane 4: whole cell of E3-E01-A02; Lane 5: whole cell of E4-E01-A02; Lane 6: whole cell of E5-E01-A02. M: protein molecular weight marker.

Supplementary Figure 4—Cell growth of engineered strains.

Declarations

Conflict of interest The authors declare that they have no conflict of interest.

References

Albertsen L, Chen Y, Bach LS, Rattleff S, Maury J, Brix S, Nielsen J, Mortensen UH (2011) Diversion of flux toward sesquiterpene production in *Saccharomyces cerevisiae* by fusion of host and heterologous enzymes. Appl Environ Microbiol 77:1033–1040

Brower PL, Butler DE, Deering CF, Le TV, Millar A, Nanninga TN, Roth D (1992) The synthesis of (4R-cis)-1,1-dimethylethyl 6-cyanomethyl-2,2-dimethyl-1,3-dioxane-4-acetate, a key intermediate for the preparation of CI-981, a highly potent, tissue selective inhibitor of HMG-CoA reductase. Tetrahedron Lett 33:2279–2282

Chen K, Li K, Deng J, Zhang B, Lin J, Wei D (2016) Carbonyl reductase identification and development of whole-cell biotransformation for highly efficient synthesis of (R)-[3,5-bis(trifluoromethyl)phenyl] ethanol. Microb Cell Fact 15:191

Choi KY, Wernick DG, Tat CA, Liao JC (2014) Consolidated conversion of protein waste into biofuels and ammonia using *Bacillus subtilis*. Metab Eng 23:53–61

Choi S, Song CW, Shin JH, Lee SY (2015) Biorefineries for the production of top building block chemicals and their derivatives. Metab Eng 28:223–239

Corey EJ, Niwa H, Knolle J (1978) Total synthesis of (S)-12-hydroxy-5,8,14-cis-10-trans-eicosatetraenoic acid (Samuelesson's HETE). J Am Chem Soc 100(6):1942–1944

Dhamankar H, Tarasova Y, Martin CH, Prather KLJ (2014) Engineering *E. coli* for the biosynthesis of 3-hydroxy-γ-butyrolactone (3HBL) and 3,4-dihydroxybutyric acid (3,4-DHBA) as value-added chemicals from glucose as a sole carbon source. Metab Eng 25:72–81

Hollingsworth RI (1994) Process for the preparation of 3,4-dihydroxybutanoic acid and salts thereof. European Patent Office Publ. of Application with search report EP19910114350

Inoue K, Matsumoto M, Takahashi S (1991) Method of preparing optically active 3,4-dihydroxy butyric acid derivatives. European Patent Office Publ. of Application with search report EP0339618 B1

Kawaguchi H, Hasunuma T, Ogino C, Kondo A (2016) Bioprocessing of bio-based chemicals produced from lignocellulosic feedstocks. Curr Opin Biotechnol 42:30–39

Kim EE, Baker CT, Dwyer MD, Murcko MA, Rao BG, Tung RD, Navia MA (1995) Crystal structure of HIV-1 protease in complex with VX-478, a potent and orally bioavailable inhibitor of the enzyme. J Am Chem Soc 117(3):1181–1182

Li J, Zhang R, Xu Y, Xiao R, Li K, Liu H, Jiang J, Zhou X, Li L, Zhou L (2017) Ala258Phe substitution in *Bacillus sp.* YX-1 glucose dehydrogenase improves its substrate preference for xylose. Process Biochem 56:124–131

Liu XW, Wang HH, Chen JY, Li XT, Chen GQ (2009) Biosynthesis of poly(3-hydroxybutyrate-co-3-hydroxyvalerate) by recombinant *Escherichia coli* harboring propionyl-CoA synthase gene (prpE) or propionate permease gene (prpP). Biochem Eng J 43:72–77

Lu P, Feng MG, Li WF, Hu CX (2006) Construction and characterization of a bifunctional fusion enzyme of *Bacillus*-sourced beta-glucanase and xylanase expressed in *Escherichia coli*. FEMS Microbiol Lett 261:224–230

Ryosuke F, Shuhei N, Tsutomu T, Akihiko K (2018) Muconic acid production using gene-level fusion proteins in *Escherichia coli*. ACS Synth Biol 7(11):2698–2705

Sang HP, Lee SH, Sang YL (2010) Preparation of optically active β-amino acids from microbial polyester polyhydroxyalkanoates. J Chem Res 2001:498–499

Schweiger G, Buckel W (1984) On the dehydration of (R)-lactate in the fermentation of alanine to propionate by *Clostridium propionicum*. FEBS Lett 171:79–84

Shieh HM, Prestwich GD (1982) Chiral, biomimetic total synthesis of(-)-aplysistatin. Tetrahedron Lett 23(45):4643–4646

Sivaramakrishnan S, Spudich JA (2011) Systematic control of protein interaction using a modular ER/K α-helix linker. Proc Natl Acad Sci USA 108(51):20467–20472

Sun L, Yang F, Sun HB, Zhu TC, Li XH, Li Y, Xu ZH, Zhang YP (2016) Synthetic pathway optimization for improved 1,2,4-butanetriol production. J Ind Microbiol Biotechnol 43:67–78

Taguchi S, Yamada M, Matsumoto K, Tajima K, Satoh Y, Munekata M, Ohno K, Kohda K, Shimamura T, Kambe H (2008) A microbial factory for lactate-based polyesters using a lactate-polymerizing enzyme. Proc Natl Acad Sci 105:17323–17327

Tetrahedron M (1990) Enantiomerically pure β, γ-epoxyesters from β-hydroxylactones: synthesis of β-hydroxyesters and (-)-GABOB. Tetrahedron 46:4277–4282

Valdehuesa KNG, Liu H, Ramos K, Si JP, Nisola GM, Lee WK, Chung WJ (2014) Direct bioconversion of d -xylose to 1,2,4-butanetriol in an engineered *Escherichia coli*. Process Biochem 49:25–32

Wang J, Shen X, Jain R, Wang J, Yuan Q, Yan Y (2017) Establishing a novel biosynthetic pathway for the production of 3,4-dihydroxybutyric acid from xylose in *Escherichia coli*. Metab Eng 41:39–45

Zhong WQ, Zhang Y, Wu WJ, Liu DH, Chen Z (2019) Metabolic engineering of a homoserine-derived non-natural pathway for the De Novo production of 1,3-propanediol from glucose. ACS Synth Biol 8:587–595